Spin-resolved second-order correlation energy of the two-dimensional uniform electron gas

Michael Seidl
Institute of Theoretical Physics, University of Regensburg, D-93040 Regensburg, Germany
(Received 9 December 2003; revised manuscript received 19 May 2004; published 13 August 2004)

For the two-dimensional (2D) electron gas, the leading term in the high-density limit of the correlation energy is evaluated here numerically for all values of the spin polarization. The result is spin-resolved into $\uparrow\uparrow$, $\uparrow\downarrow$, and $\downarrow\downarrow$ contributions and parametrized analytically. Interaction-strength interpolation yields a local spin-density functional (LSD) for the correlation energy in 2D at finite densities.

DOI: 10.1103/PhysRevB.70.073101 PACS number(s): 71.10.−w, 73.20.−r

In recent years, two-dimensional (2D) electron systems have become the subject of extensive research.[1] The 2D version of density functional theory (DFT) has proven particularly successful in studying quantum dots.[2–4] The local spin-density approximation (LSD) of DFT requires the correlation energy of the spin-polarized uniform electron gas. This quantity in 2D is known accurately for a wide range of densities and spin polarizations from fixed-node diffusion Monte Carlo simulations.[5] Its high-density limit is known exactly in terms of six-dimensional momentum-space integrals.[6] Resolved into contributions due to $\uparrow\uparrow$, $\uparrow\downarrow$, and $\downarrow\downarrow$ excitation electron pairs, these integrals are evaluated here numerically. The analytical parametrization of the results, Eqs. (16) and (17) below, is a crucial ingredient for the construction of the spin-resolved correlation energy at finite densities, performed recently for the 3D electron gas.[7] It is also required for studying the magnetic response of the spin-polarized 2D electron gas.[8,9] Generally, it provides a fundamental test for numerical parametrizations of the correlation energy.[5]

In the 2D uniform electron gas, the electrons are moving on a plane at uniform density $\rho=[\pi(r_s a_B)^2]^{-1}$, where $a_B=0.529$ Å is the Bohr radius and r_s is the dimensionless density parameter (Seitz radius). We consider lowest-energy states with a given spin polarization

$$\zeta \equiv \frac{\rho_\uparrow - \rho_\downarrow}{\rho}, \tag{1}$$

where $\rho_\uparrow$ and $\rho_\downarrow \equiv \rho - \rho_\uparrow$, respectively, are the (uniform) densities of spin-up and spin-down electrons. Including a neutralizing positive background, the total energy per electron is a unique function of the dimensionless parameters r_s and ζ,

$$e_{tot}(r_s,\zeta) = t_s(r_s,\zeta) + e_x(r_s,\zeta) + e_c(r_s,\zeta). \tag{2}$$

The noninteracting kinetic and exchange energies,

$$t_s(r_s,\zeta) = \frac{1+\zeta^2}{2}\frac{1}{r_s^2},$$

$$e_x(r_s,\zeta) = -\frac{4\sqrt{2}}{3\pi}\frac{(1+\zeta)^{3/2}+(1-\zeta)^{3/2}}{2}\frac{1}{r_s} \tag{3}$$

(all energies are given in units of 1 Ha $\equiv e^2/a_B = 27.21$ eV in the following), may be understood as the zeroth- and the first-order terms of a perturbation expansion for the quantity $r_s^2 e_{tot}(r_s,\zeta)$ with respect to the electron-electron interaction (where r_s turns out to be the expansion parameter).

The remaining *correlation energy* in Eq. (2) appears to have the perturbation (high-density) expansion[10,11]

$$e_c(r_s,\zeta) = \sum_{n=0}^{\infty} [a_n(\zeta)\ln(r_s) + b_n(\zeta)] r_s^n \quad (r_s \ll 1). \tag{4}$$

For the 2D electron gas (but not for the 3D one), the first coefficient vanishes, $a_0(\zeta)\equiv 0$. Consequently, the "second-order" term ($n=0$) is $e_c^{(2)}(\zeta) \equiv b_0(\zeta)$, representing the high-density ($r_s \to 0$) limit of $e_c(r_s,\zeta)$. It can be split into an exchange ("2b") and a ring-diagram ("2r") term,[6]

$$e_c^{(2)}(\zeta) = e_c^{(2b)} + e_c^{(2r)}(\zeta). \tag{5}$$

The exchange term has only equal-spins contributions, $e_c^{(2b)} = e_{c\uparrow\uparrow}^{(2b)}(\zeta) + e_{c\downarrow\downarrow}^{(2b)}(\zeta)$, given by the $\delta_{\sigma_1\sigma_2}$ term of Eq. (14) in Ref. 6 (we choose the k_x axis in the direction of $\mathbf{q}$),

$$e_{c,\sigma\sigma}^{(2b)}(\zeta) = \frac{1}{8\pi^2}\int_0^\infty \frac{dq}{q} \int_{A[\kappa_\sigma(\zeta),q]} d^2k_1 \int_{A[\kappa_\sigma(\zeta),q]} d^2k_2 \times \frac{1}{|q\mathbf{e}_x + \mathbf{k}_1 + \mathbf{k}_2|}\frac{1}{q + k_{1x} + k_{2x}}. \tag{6}$$

Here, q, $\mathbf{k}_1$, and $\mathbf{k}_2$ are dimensionless, $\sigma \in \{\uparrow,\downarrow\}$, and the domain of the 2D integrals is

$$A[\kappa,q] \equiv \{\mathbf{k}\in \mathrm{R}^2 | |\mathbf{k}| < \kappa, |\mathbf{k}+q\mathbf{e}_x| > \kappa\},$$

$$\kappa_\sigma(\zeta) \equiv [1+\mathrm{sgn}(\sigma)\zeta]^{1/2}. \tag{7}$$

[$\kappa_\sigma(\zeta)$ is the Fermi wave vector for spin-σ electrons in units of its value at $\zeta=0$.] Scaling the integration variables by some constant κ, $q=\kappa Q$ and $\mathbf{k}=\kappa\mathbf{K}$, we have generally

$$\int_0^\infty \frac{dq}{q}\int_{A[\kappa,q]} d^2k f(q,\mathbf{k}) = \kappa^2 \int_0^\infty \frac{dQ}{Q}\int_{A[1,Q]} d^2K f(\kappa Q, \kappa\mathbf{K}). \tag{8}$$

Applying this rule to the integrals in Eq. (6), we find[6]

$$e_{c,\sigma\sigma}^{(2b)}(\zeta) = [1+\mathrm{sgn}(\sigma)\zeta] J^{(2b)}. \tag{9}$$

Consequently,[6] the full second-order exchange term $e_c^{(2b)} = e_{c\uparrow\uparrow}^{(2b)}(\zeta) + e_{c\downarrow\downarrow}^{(2b)}(\zeta) \equiv 2J^{(2b)}$ is ζ-independent. A Monte Carlo integration yields

$$J^{(2b)} \equiv e_{c\uparrow\uparrow}^{(2b)}(0) = (57.15 \pm 0.05)\text{mHa} \quad (1\ \text{mHa} = 10^{-3}\ \text{Ha}). \tag{10}$$

The ring-diagram term $e_c^{(2r)}(\zeta)$ is the remaining part of expression (14) in Ref. 6, with the contributions

$$e_{c,\sigma_1\sigma_2}^{(2r)}(\zeta) = -\frac{1}{8\pi^2}\int_0^\infty \frac{dq}{q^2} \int_{A[\kappa_{\sigma_1}(\zeta),q]} d^2k_1 \times \int_{A[\kappa_{\sigma_2}(\zeta),q]} d^2k_2 \frac{1}{q + k_{1x} + k_{2x}}. \tag{11}$$

The equal-spins terms ($\sigma_1 = \sigma_2$) can be treated in the same way as the integral (6),

$$e_{c,\sigma\sigma}^{(2r)}(\zeta) = -[1 + \text{sgn}(\sigma)\zeta]J^{(2r)}, \quad J^{(2r)} = (76.69 \pm 0.03)\text{mHa}. \tag{12}$$

The only nontrivial ζ-dependence is in the opposite-spins term $e_{c\uparrow\downarrow}^{(2r)}(\zeta) \equiv e_{c\downarrow\uparrow}^{(2r)}(\zeta)$,

$$e_{c\uparrow\downarrow}^{(2r)}(\zeta) = e_{c\uparrow\downarrow}^{(2r)}(0)[1 - f(\zeta)]. \tag{13}$$

By definition, $f(0) = 0$, and, since $e_{c\uparrow\downarrow}^{(2r)}(1) = 0$, $f(1) = 1$. Moreover, $e_{c\uparrow\downarrow}^{(2r)}(0) = -J^{(2r)}$. When the results of a Monte Carlo evaluation of $f(\zeta)$ at different values of ζ are compared with the functions $f_\alpha(\zeta) \equiv [(1+\zeta)^\alpha + (1-\zeta)^\alpha - 2]/(2^\alpha - 2)$, particularly good agreement (specially for $\zeta \to 0$ and $\zeta \to 1$) is found in the limit $\alpha \to 1$ [Fig. 1(a)],

$$f(\zeta) = f_1(\zeta) + \delta f(\zeta),$$

$$f_1(\zeta) \equiv \frac{(1+\zeta)\ln(1+\zeta) + (1-\zeta)\ln(1-\zeta)}{2\ln 2}. \tag{14}$$

The choice of the functions $f_\alpha(\zeta)$ is motivated by the observation that they also describe the ζ-dependence of $t_s(r_s,\zeta)$ and $e_x(r_s,\zeta)$ in Eq. (3),

$$g(r_s,\zeta) = g(r_s,0) + [g(r_s,1) - g(r_s,0)]f_\alpha(\zeta),$$

where $\alpha = 2$ for $g = t_s$ and $\alpha = \frac{3}{2}$ for $g = e_x$. [In the case of Eq. (13), note that $g(r_s,1) = 0$.] The small deviation $\delta f(\zeta)$ in Eq. (14) is accurately fitted by a polynomial [Fig. 1(b)]

$$\delta f(\zeta) \approx 0.0636\zeta^2 - 0.1024\zeta^4 + 0.0389\zeta^6. \tag{15}$$

The small minimum of $\delta f(\zeta)$ indicated by the numerical data [dots in Fig. 1(b)] at $\zeta \approx 0.98$ is probably real, since a similar peculiarity is observed in the case of the 3D electron gas (see the inset in Fig. 1 of Ref. 12).

In summary, the second-order correlation energy $e_c^{(2)}(\zeta) = e_c^{(2b)} + e_c^{(2r)}(\zeta)$ is

$$e_c^{(2)}(\zeta) \equiv e_{c\uparrow\uparrow}^{(2)}(\zeta) + 2e_{c\uparrow\downarrow}^{(2)}(\zeta) + e_{c\downarrow\downarrow}^{(2)}(\zeta) = [153.38 f(\zeta) - 192.46]\text{mHa}, \tag{16}$$

where $f(\zeta)$ is given by Eqs. (14) and (15). The spin resolution is fixed by

$$e_{c\uparrow\uparrow}^{(2)}(\zeta) \equiv e_{c\downarrow\downarrow}^{(2)}(-\zeta) = -(1+\zeta) \times 19.54\ \text{mHa}. \tag{17}$$

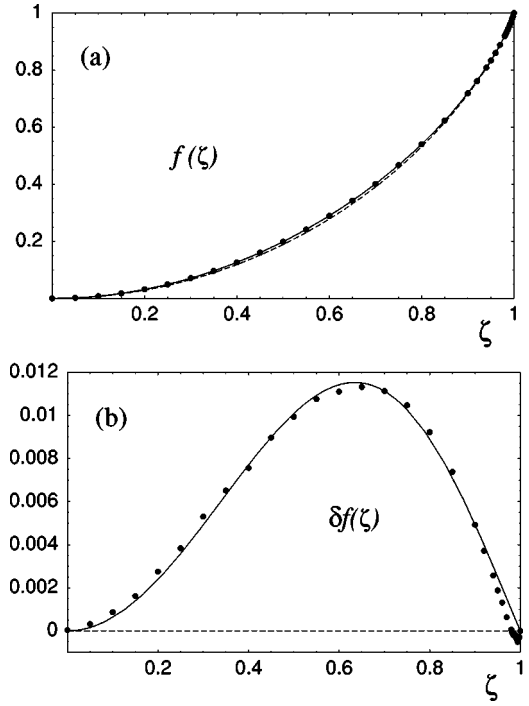

FIG. 1. (a) Numerical results (dots) for the function $f(\zeta)$ of Eq. (13) obtained by Monte Carlo integrations of expression (11) (with $\sigma_1\sigma_2 = \uparrow\downarrow$) at selected values of ζ. The analytical function $f_1(\zeta)$ of Eq. (14) is plotted as a dashed curve. The solid curve represents the accurate fit $f_1(\zeta) + \delta f(\zeta)$, using Eq. (15) for $\delta f(\zeta)$. (b) The fit (15) (solid curve) compared to the true deviation (dots) of the Monte Carlo integration results from $f_1(\zeta)$.

$e_c^{(2)}(\zeta) \equiv e_c(0,\zeta)$ is the *high-density* limit $r_s \to 0$ of the full correlation energy $e_c(r_s,\zeta)$. To illustrate the relevance of this limit for finite densities ($r_s > 0$), the present result can be used in the interaction-strength interpolation (ISI) of Ref. 13. This approach does not require the higher-order ($n \geqslant 1$) terms of the expansion (4) (which is expected to have only a finite radius of convergence). Instead, information beyond the second order is taken from the opposite low-density (strong-interaction or Wigner-crystal) limit of the exchange-correlation energy $e_{xc} \equiv e_x + e_c$ (per electron),

$$e_{xc}(r_s,\zeta) \to \frac{a_\infty}{r_s} + \frac{b_\infty}{r_s^{3/2}} \quad (r_s \to \infty). \tag{18}$$

The coefficients[14] $a_\infty \approx -1.1061$ and $b_\infty \approx \frac{1}{2}$ are independent of ζ, since any spatial overlap between two electrons is strongly suppressed in this limit, no matter whether their spins are parallel or not.[15] The resulting ISI expression for the exchange-correlation energy at finite densities reads[13]

$$e_{xc}^{ISI}(r_s,\zeta) = \frac{a_\infty}{r_s} + \frac{2X}{Y}\left[(1+Y)^{1/2} - 1 - Z\ln\left(\frac{(1+Y)^{1/2} + Z}{1+Z}\right)\right]. \tag{19}$$

Using $b_\infty = \frac{1}{2}$ and writing $e_x(r_s,\zeta) = c_x(\zeta)/r_s$, we have explicitly[13]

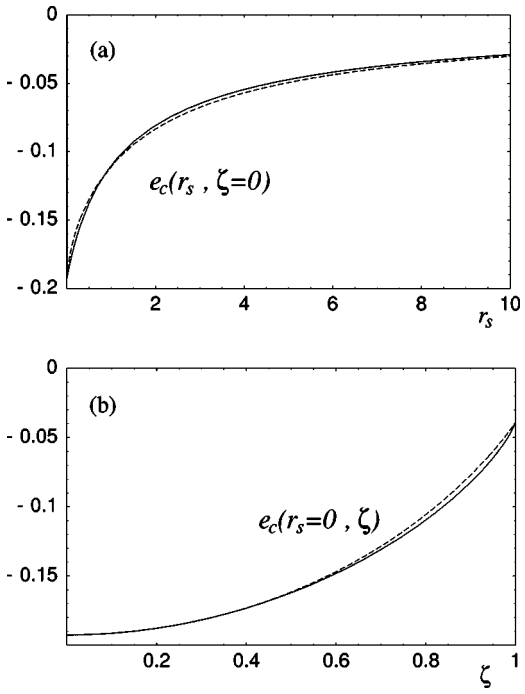

FIG. 2. The correlation energy of Ref. 5 (dotted curves) versus the present ISI results (solid curves); energies are in hartree units.

$$X(r_s,\zeta) = \frac{-e_c^{(2)}(\zeta)}{[c_x(\zeta)-a_\infty]^2}\frac{1}{r_s},$$

$$Y(r_s,\zeta) = \frac{4e_c^{(2)}(\zeta)^2}{[c_x(\zeta)-a_\infty]^4}r_s,$$

$$Z(\zeta) = \frac{-e_c^{(2)}(\zeta)}{[c_x(\zeta)-a_\infty]^3} - 1. \qquad (20)$$

In Fig. 2(a), the ISI prediction $e_c^{ISI}(r_s,\zeta)=e_{xc}^{ISI}-e_x$ for the correlation energy of the unpolarized uniform electron gas ($\zeta=0$) is compared with the accurate parametrization of the fixed-node diffusion Monte Carlo results in Ref. 5. e_c^{ISI} differs slightly from the latter by up to 4%. This mild deviation might be cured by including in the ISI a simple model for the next-order coefficient of expansion (4).[16] In the high-density limit ($r_s\to 0$), however, where the present result is virtually exact, the parametrization in Ref. 5 has for $0.7<\zeta<0.95$ a small positive deviation,[5] shown in Fig. 2(b).

Reference 5 predicts a sudden transition into a fully polarized ground state for $r_s>25.56$. In the present model, the total energy per electron, $e_{tot}^{ISI}(r_s,\zeta)=t_s+e_{xc}^{ISI}$, becomes lower for $\zeta=1$ than for $\zeta=0$ at $r_s\approx 6.3$. More precisely, Fig. 3(a) shows the difference $e_{tot}^{ISI}(r_s,\zeta)-e_{tot}^{ISI}(r_s,0)$ versus ζ at different values of r_s. Due to this figure, nearly full polarization $\zeta\approx 0.95$ would be energetically favorable already at $r_s=6.0$. A corresponding divergence in the spin susceptibility $\chi(r_s)$

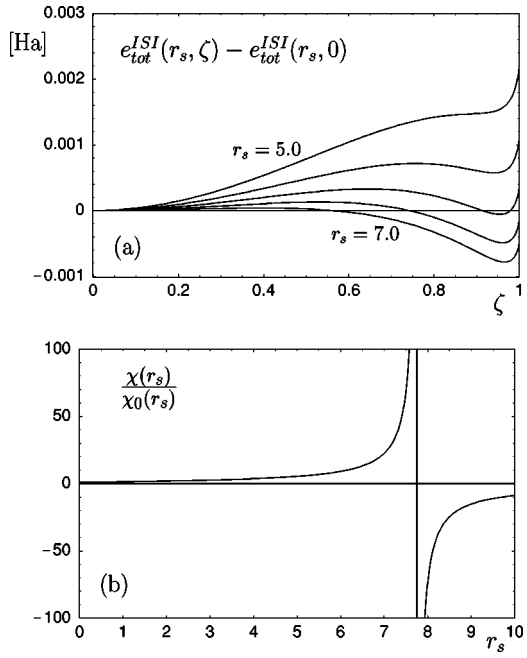

FIG. 3. (a) The difference in ISI total energy per electron between the state with polarization ζ and the unpolarized state ($\zeta=0$) for (from top to bottom) $r_s=5.0, 5.5, 6.0, 6.5, 7.0$. (b) The spin susceptibility $\chi(r_s)\equiv[\partial^2 e_{tot}^{ISI}(r_s,\zeta)/\partial\zeta^2]^{-2}|_{\zeta=0}$ in units of its noninteracting value $\chi_0(r_s)\equiv[\partial^2 t_s(r_s,\zeta)/\partial\zeta^2]^{-1}|_{\zeta=0}=r_s^2$.

occurs at $r_s\approx 7.8$ [Fig. 3(b)]. These results demonstrate that the present model (19) qualitatively predicts the correct magnetic transition, but at a density which is too high. Better accuracy might be achieved if higher-order terms of the high-density expansion (4) are included. As pointed out in Ref. 5, however, this transition is very subtle [note the small energy scale in Fig. 3(a)] and approximate predictions for its density tend to be too high.[17]

Conclusions: The high-density limit, given by Eq. (16), of the correlation energy $e_c(r_s,\zeta)$ in the 2D uniform electron gas provides a strong test for the results of Monte Carlo computations.[5] Moreover, Eq. (16) is a basic ingredient for constructing 2D density functionals. For example, extrapolation to the low-density limit yields a simple estimate (19) for $e_c(r_s,\zeta)$. Even the subtle transition to a ferromagnetic ground state is predicted qualitatively correctly. For arbitrary *nonuniform* 2D electron systems (such as quantum dots) with local densities $\rho_\uparrow(\mathbf{r})$ and $\rho_\downarrow(\mathbf{r})$ of spin-up and spin-down electrons, respectively, Eq. (19) provides an explicit local spin-density approximation (LSD),

$$E_{xc}^{LSD}[\rho_\uparrow,\rho_\downarrow] = \int d^2r\rho(\mathbf{r})e_{xc}^{ISI}(r_s(\mathbf{r}),\zeta(\mathbf{r})), \qquad (21)$$

for treatment by the Kohn–Sham equations of DFT. In Eq. (21), $r_s(\mathbf{r})=a_B^{-1}[\pi\rho(\mathbf{r})]^{-1/2}$, $\rho(\mathbf{r})=\rho_\uparrow(\mathbf{r})+\rho_\downarrow(\mathbf{r})$, and $\zeta(\mathbf{r})=[\rho_\uparrow(\mathbf{r})-\rho_\downarrow(\mathbf{r})]/\rho(\mathbf{r})$.

[1] E. Abrahams, S. V. Kravchenko, and M. P. Sarachik, Rev. Mod. Phys. **73**, 251 (2001).
[2] S. M. Reimann and M. Manninen, Rev. Mod. Phys. **74**, 1283 (2002).
[3] H. Jiang, H. U. Baranger, and W. Yang, Phys. Rev. B **68**, 165337 (2003).
[4] H. Saarikoski, E. Räsänen, S. Siljamäki, A. Harju, M. J. Puska, and R. M. Nieminen, Phys. Rev. B **67**, 205327 (2003).
[5] C. Attaccalite, S. Moroni, P. Gori-Giorgi, and G. B. Bachelet, Phys. Rev. Lett. **88**, 256601 (2002).
[6] A. K. Rajagopal and J. C. Kimball, Phys. Rev. B **15**, 2819 (1977).
[7] P. Gori-Giorgi and J. P. Perdew, Phys. Rev. B **69**, 041103(R) (2004).
[8] J. Moreno and D. C. Marinescu, Phys. Rev. B **68**, 195210 (2003).
[9] M. Polini and M. P. Tosi, Phys. Rev. B **63**, 045118 (2001).
[10] W. Macke, Z. Naturforsch. A **5A**, 192 (1950).
[11] W. J. Carr and A. A. Maradudin, Phys. Rev. **133**, A371 (1964).
[12] G. G. Hoffman, Phys. Rev. B **45**, 8730 (1992).
[13] M. Seidl, J. P. Perdew, and S. Kurth, Phys. Rev. Lett. **84**, 5070 (2000).
[14] L. Bonsall and A. A. Maradudin, Phys. Rev. B **15**, 1959 (1977).
[15] M. Seidl, J. P. Perdew, and S. Kurth, Phys. Rev. A **62**, 012502 (2000).
[16] M. Seidl and J. P. Perdew (unpublished).
[17] S. Yarlagadda and G. F. Giuliani, Phys. Rev. B **40**, 5432 (1989).